# Evaluation of the MPD/NICA detector capabilities for studies of hyperon production in HIC

*Veronika Vasendina, Alexander Zinchenko* for the MPD Collaboration

JINR, 141980 Dubna, Moscow region, Russia

**DOI:** http://dx.doi.org/10.3204/DESY-PROC-2014-04/178

One of the main tasks of NICA/MPD physics program is a study of the strangeness production in nuclear collisions. In this paper the MPD detector performance for measurements of $\Lambda$, $\bar{\Lambda}$, $\Xi^-$, $\bar{\Xi}^+$, $\Omega^-$ and $\bar{\Omega}^+$ hyperons in central Au+Au collisions at NICA energies is presented.

## 1 Introduction

The main goal of studying heavy-ion collisions is to explore the properties of nuclear matter under extreme density and temperature conditions. Production of strange particles is of particular interest because enhanced production of rare strange hadrons ($\Xi^-$, $\bar{\Xi}^+$, $\Omega^-$, $\bar{\Omega}^+$), in A+A collisions (relative to the yields from elementary pp reactions) was predicted as a signal for the QGP formation [1].

At present, a complete theoretical description of the (multi)strangeness production mechanism at collision energies ($\sqrt{s}$) of several GeV has not yet been achieved. In order to better understand the dynamics of hot and dense hadronic matter the MPD experiment at NICA [2] will provide new precise experimental data on the total yields, rapidity, transverse momentum, and azimuthal angle distributions of hyperons. The production of baryons and antibaryons with different strangeness content in central heavy ion collisions will be compared with that in proton induced reactions where no QGP formation is expected.

The goal of this study is to evaluate the performance of the MPD detector for reconstruction of hyperons in Au+Au collisions.

## 2 MPD detector: geometry, event reconstruction and particle identification

The detailed description of the MPD geometry can be found in Refs. [2, 3, 4]. The present analysis is based on the detectors covering the mid-rapidity region ($|\eta| < 1.3$): the main tracker Time Projection Chamber (TPC) and barrel Time-Of-Flight system (TOF), comprising a so-called start version. The overall detector material budget is dominated by the contribution from the TPC inner and outer cages which are multilayer structures made of composite materials like kevlar and tedlar with high strength and long radiation length. As a result, the total amount of the material does not exceed 10% of the radiation length in the region of interest.

The track reconstruction method is based on the Kalman filtering technique (see, e.g. [5]) and the number of TPC points per track was required to be greater than 10 to ensure a good precision of momentum and $dE/dx$ measurements. In addition, we have restricted our study to the mid-rapidity region with $|\eta|$ <1.3. The track finding efficiency in TPC for primary and secondary tracks is shown in Fig. 1 as a function of the track transverse momentum. The transverse momentum resolution as a function of $p_T$ can be seen on the right panel of Fig. 1. The result has been obtained with the assumption on the TPC coordinate resolution of 0.5 and 1.0 mm in transverse and longitudinal directions, respectively.

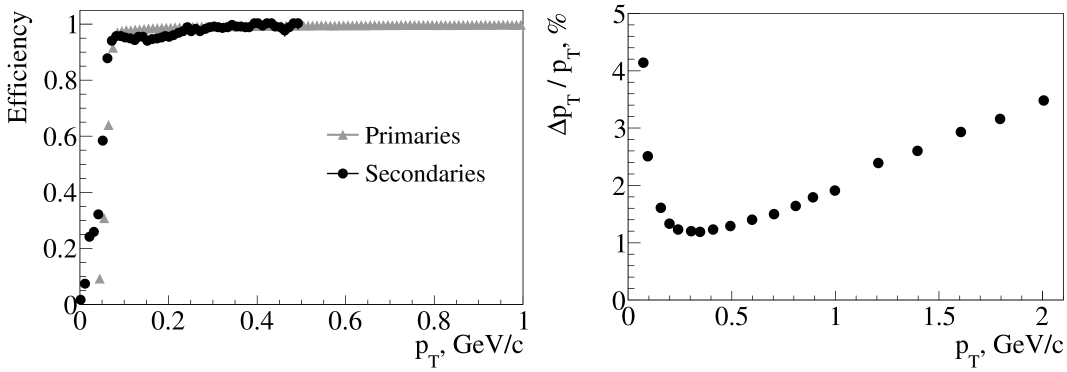


Figure 1: Track reconstruction efficiency as a function of track $p_T$ for primary and secondary particles (left); relative transverse momentum resolution for primary tracks with $|\eta|$ <1.3 reconstructed in TPC (right).

The reconstructed tracks served as an input to the primary and secondary vertex reconstruction procedures based on the Kalman filtering formalism [6].

For all the reconstructed in the TPC tracks the specific energy loss $dE/dx$ is calculated as a truncated mean of the charges of TPC hits assigned to the tracks. The truncation level of 70% was chosen, i.e. 30% of hits with the highest charges were excluded from the mean value.

Next, the TPC reconstructed tracks are extrapolated to the TOF detector and matched to the TOF hits. For the matched candidates the mass square ($M^2$) is derived through the relation:

$$M^2 = (p/q)^2 \left( \frac{c^2 t^2}{l^2} - 1 \right)$$

where $p$ is the track momentum, $q$ is its charge, $t$ is the time-of-flight from TOF, $l$ is the path length from the collision vertex to the TOF hit, and $c$ is the speed of light.

Particle identification (PID) in the MPD experiment will be achieved by combining specific energy loss ($dE/dx$) and time-of-flight measurements. The basic detector parameters, namely, $dE/dx$ and TOF resolutions of $\sigma_{dE/dx} \approx 6\%$ and $\sigma_{TOF} \approx 100$ ps will provide a high degree of selectivity for hadrons at momenta below 2 GeV/$c$.

An identified hadron candidate is assumed to lie within the boundaries of the PID ellipse ($3\sigma$ around the nominal position for a given particle specie) in the $dE/dx - M^2$ space . In addition, the probability for a given particle to belong to each of the species can be calculated knowing the widths of the corresponding distributions (along the $dE/dx$ and $M^2$ axes) and the difference from the predicted position for the specie. It was found that by requiring this probability to be greater than 0.75 one can obtain high PID efficiency and low contamination.

# 3 Simulations: event generator, data sets and results

The software framework for the MPD experiment (MpdRoot [7]) is based on FairRoot and provides a powerful tool for detector performance studies, development of algorithms for reconstruction and physics analysis of the data [2]. The event samples used for the present study were produced with the UrQMD [8] generator at $\sqrt{s} = 9$A GeV.

Produced by the event generators particles have been transported through the detector using the GEANT3 transport package (describing particle decays, secondary interactions, etc.).

Multistrange hyperons were reconstructed using their decay modes into a charged particle and a $\Lambda$ hyperon followed by $\Lambda$ decay into a proton and a pion. The event topology (decay of a relatively long-lived particle into two particles) defines the selection criteria: relatively large distance of the closest approach ($DCA$) to the primary vertex of decay products, small track-to-track separation in the decay vertex, relatively large decay length of the mother particle. Moreover, both the $DCA$ and two-track separation cuts should be more efficient if applied in $\chi^2$ - space, i.e if normalized to their respective errors.

For $\Xi^{\pm}$ ($\Omega^{\pm}$) $\Lambda$-candidates in the invariant mass interval $\pm 3\sigma$ around the peak position were combined with negative pions (kaons) to form $\Xi^{\pm}$ ($\Omega^{\pm}$)-candidates. In the selection procedure, additional acceptance cuts were introduced to find the significance maximum for this cascade decay topology.

The results for hyperon simulations (Figs. 2-4) have been obtained for $10^4$ to $5 \cdot 10^5$ central events, corresponding to about 30 seconds - 28 minutes of running time at the NICA collision rate of 6 kHz [9].

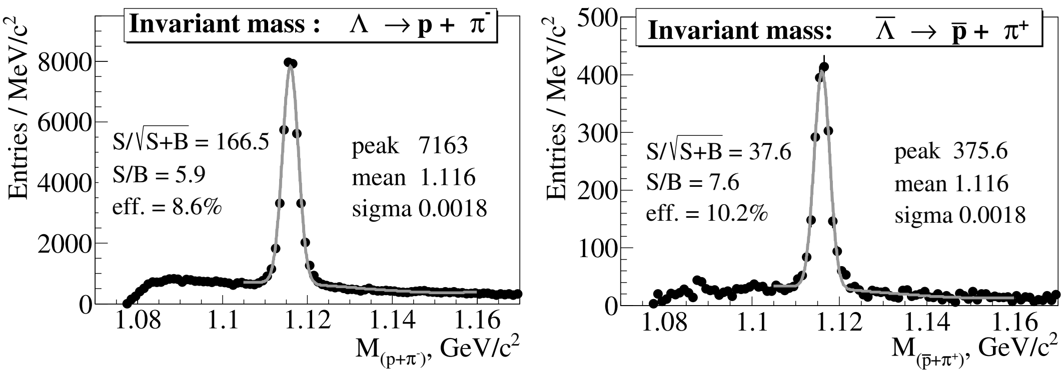


Figure 2: Reconstructed invariant mass of proton (antiproton) and $\pi^-$ ($\pi^+$).

During the selection procedure we observed a large drop in the overall reconstruction efficiency when the low-$p_T$ cut-off of decay products was increased from 0.1 to 0.2 GeV/$c$. Therefore, keeping the MPD detector ability of reconstructing very low momentum particles (at least, down to $p_T = 0.1$ GeV/$c$ - see left panel of Fig. 1) is of crucial importance for measurements of multistrange hyperons.

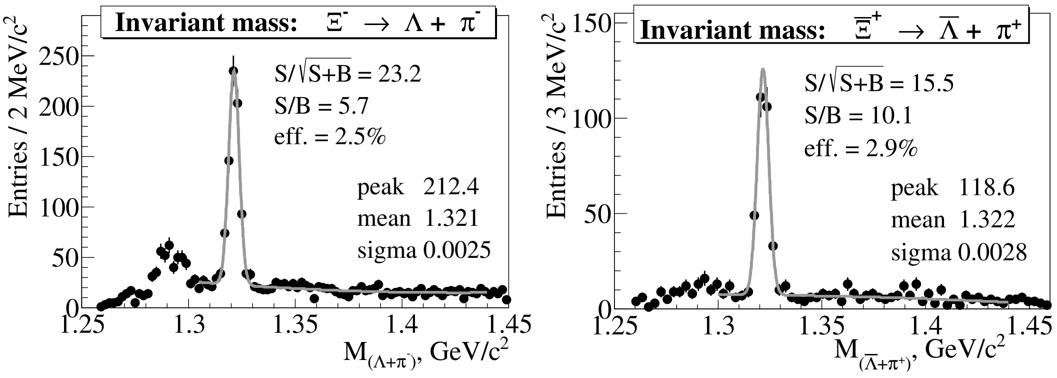


Figure 3: Reconstructed invariant mass of $\Lambda$ ($\bar{\Lambda}$) candidate and $\pi^-$ ($\pi^+$).

In conclusion we can mention that the current design of the MPD/NICA detector will make it possible to reconstruct (multi)strange hyperons in central Au+Au collisions with the invariant mass resolution of $\lesssim$3.5 MeV/$c^2$, efficiency above 1% and signal-to-background ratio $S/B \gtrsim 6$.

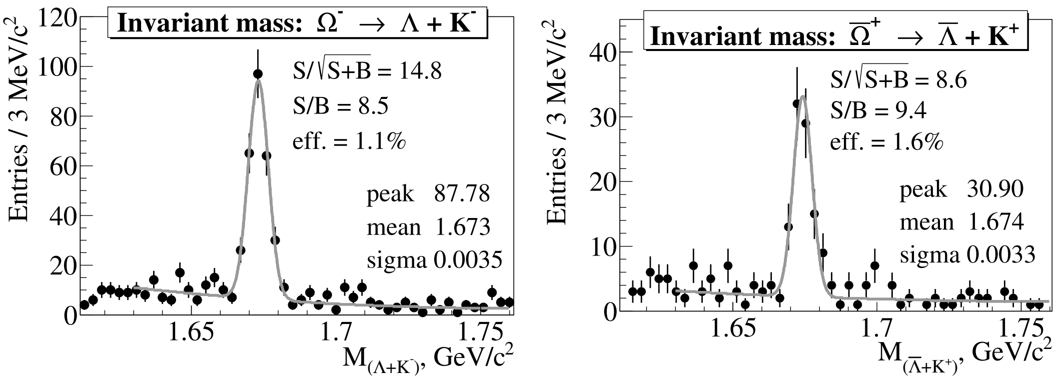


Figure 4: Reconstructed invariant mass of $\Lambda$ ($\bar{\Lambda}$) candidate and $K^-$ ($K^+$).

# References


[1] J. Rafelski and B. Mulle, Phys. Rev. Lett. **48** 1066 (1982).

[2] K. U. Abraamyan et al., Nucl. Instrum. Meth. **A628** 99 (2011).

[3] http://nica.jinr.ru/files/CDR_MPD/MPD_CDR_en.pdf.

[4] A. Zinchenko, these Proceedings.

[5] R. Fruehwirth, Nucl. Instr. and Meth. **A262** 444 (1987).

[6] R. Luchsinger and Ch. Grab, Comp. Phys. Comm., **76** 263 (1993).

[7] http://mpd.jinr.ru/.

[8] http://urqmd.org/.

[9] http://nica.jinr.ru.